Synthesis, Structure, and Photophysical Properties of Novel Ruthenium(II) Carboxypyridine Type Complexes

Thomas Norrby, Anna Börje, and Björn Åkermark*

Organic Chemistry, Department of Chemistry, Royal Institute of Technology, S-100 44 Stockholm, Sweden

Leif Hammarström and Jan Alsins

Department of Physical Chemistry, University of Uppsala, Box 532, S-751 21 Uppsala, Sweden

Kianosh Lashgari and Rolf Norrestam

Department of Structural Chemistry, Arrhenius Laboratories for Natural Sciences, Stockholm University, S-106 91 Stockholm, Sweden

Jerker Mårtensson and Gunnar Stenhagen

Department of Organic Chemistry, Chalmers University of Technology, S-412 96 Göteborg, Sweden

Received May 15, 1997[⊗]

A series of Ru(II) compounds and salts have been synthesized: [Ru(6-carboxylato-bpy)$_2$] (**5**), [Ru(6-carboxylato-bpy)(tpy)]PF_6 (**9**), [Ru(tpy)$_2$]$(PF_6)_2$ (**8**), and [Ru(bpy)$_2$(Pic)]PF_6 (**11**), where 6-carboxy-bpy (**1**) = 6-carboxy-2,2′-bipyridine, tpy (**2**) = 2,2′:6′,2″-terpyridine, and Pic = 2-carboxylatopyridine. The compounds have been characterized by NMR, electrospray mass spectrometry (ESI-MS), cyclic voltammetry, absorption and emission spectroscopy (at 100, 140, and 298 K), and single-crystal X-ray diffraction (complex **5**). Complex **5** crystallizes in the monoclinic system, space group $P2_1/n$, formula $RuC_{22}H_{14}N_4O_4 \cdot C_2H_5OH$, with $a = 11.088(3)$ Å, $b = 11.226(3)$ Å, $c = 35.283(9)$ Å, $\beta = 91.41(2)°$, and $Z = 8$. A linear dependence on the number of coordinated carboxylato groups and the electrochemical redox potentials was found, ca. 0.4 V lower reduction potential for the oxidation step (Ru(II/III)) per carboxylate group. Also, to the best of our knowledge, these are the first examples (**9**, **11**) of mononuclear Ru(II) complexes containing a carboxypyridine−ruthenium moiety displaying any luminescence emission.

Introduction

During several decades, intense efforts have been devoted to the study of the photophysical, photochemical, and electrochemical properties of ruthenium and osmium polypyridine complexes, as photosensitizers in model systems for the study of photoinduced electron transfer[1] and artificial photosynthesis.[2] In these types of complexes, absorption of light generally gives rise to luminescent, relatively long-lived metal-to-ligand charge-transfer excited states, usually described as a closely spaced manifold of metal-to-ligand charge-transfer (MLCT) states of mainly triplet character (^{3}MLCT).[1a,3] In systems where this ^{3}MLCT state is sufficiently long-lived and has a suitable redox potential, it may be oxidatively quenched by various electron acceptors,[4] resulting in a photoinduced electron transfer. A systematic variation of the chemical composition of the photosensitizer leads to systematic variations in the properties found in a new compound, such as the lifetime (τ) and the emission quantum yield (Φ_{em}) of the emitting excited state, and the excited state redox potential.[1a,5]

As a part of our continued interest in the study of novel ruthenium polypyridyl compounds, we have prepared some

* To whom correspondence should be addressed. E-mail: bear@orgchem.kth.se. Fax: int. + 46-8791 23 33.

⊗ Abstract published in *Advance ACS Abstracts,* November 1, 1997.

(1) (a) Juris, A.; Balzani, V.; Barigelletti, F.; Campagna, S.; Belser, P.; von Zelewsky, A. *Coord. Chem. Rev.* **1988**, *84*, 85. (b) Balzani, V.; Juris, A.; Venturi, M.; Campagna, S.; Serroni, S. *Chem. Rev.* **1996**, *96*, 759. (c) Balzani V.; Scandola, F. *Supramolecular Photochemistry*; Ellis Horwood: Chichester, U.K., 1991. (d) Roundhill, D. M. *Photochemistry and Photophysics of Metal Complexes*; Plenum: New York, 1994. (e) Allen, G. H.; White, R. P.; Rillema, D. P.; Meyer, T. J. *J. Am. Chem. Soc.* **1984**, *106*, 2613. (f) Watts, R. J. *J. Chem. Educ.* **1983**, *60*, 834.

(2) (a) Willner, I.; Willner, B. *Top. Curr. Chem.* **1991**, *159*, 153. (b) Meyer, T. J. *Acc. Chem. Res.* **1989**, *22*, 163.

(3) (a) Meyer, T. J. *Pure Appl. Chem.* **1986**, *58*, 1193. (b) Barqawi, K. R.; Murtaza, Z.; Meyer, T. J. *J. Phys. Chem.* **1991**, *95*, 47. (c) DeArmond, M. K.; Myrick, M. L. *Acc. Chem. Res.* **1989**, *22*, 364. (d) Kalyanasundaram, K. *Photochemistry of Polypyridine and Porphyrin Complexes*; Academic Press: London, 1992; p 118.

(4) (a) Balzani, V.; Scandola, F. *Supramolecular Photochemistry*; Ellis Horwood: Chichester, U.K., 1991; Chapter 2. (b) Kalyanasundaram, K. *Photochemistry of Polypyridine and Porphyrin Complexes*; Academic Press: London, 1992; pp 142−163. (c) Hoffman, M. Z.; Bolletta, F.; Moggi, L.; Hug, G. L. *J. Phys. Chem. Ref. Data* **1989**, *18*, 219.

(5) (a) von Zelewsky, A.; Belser, P.; Hayoz, P.; Dux, R.; Hua, X.; Suckling, A.; Stoeckli-Evans, H. *Coord. Chem. Rev.* **1994**, *132*, 75. (b) Meyer, T. J. *Pure Appl. Chem.* **1990**, *62*, 1003. (c) Durham, B.; Caspar, J. V.; Nagle, J. K.; Meyer, T. J. *J. Am. Chem. Soc.* **1982**, *104*, 4803. (d) Lumpkin, R. S.; Kober, E. M.; Worl, L. A.; Murtaza, Z.; Meyer, T. J. *J. Phys. Chem.* **1990**, *94*, 239. (e) Haga. M.; Meser Ali, M.; Koseki, S.; Fujimoto; K.; Yoshimura, A.; Nozaki, K.; Ohno, T.; Nakajima; K.; Stufkens, D. J. *Inorg. Chem.* **1996**, *35*, 3335. (f) Henderson, L. J., Jr.; Fronczek, F. R.; Cherry, W. R. *J. Am. Chem. Soc.* **1984**, *106*, 5876.

S0020-1669(97)00581-8 CCC: $14.00

structures based on the ligand 6-carboxy-bpy (**1**) (bpy = 2,2′-bipyridine)[6] and tpy (**2**) (tpy = 2,2′:6′,2″-terpyridine). In these,

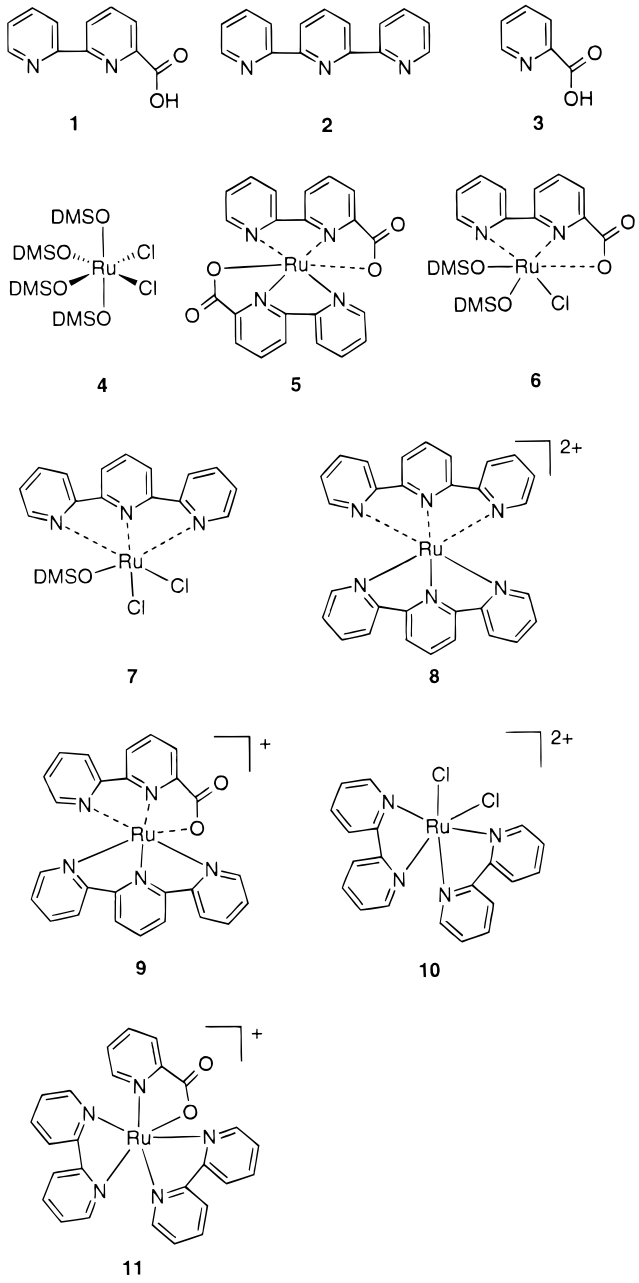

the ligand, the deprotonated form of **1**, acts as a tridentate ligand, utilizing two nitrogens and one oxygen from the carboxylate group in binding to Ru(II), and tpy as a tridentate ligand with three binding nitrogens. Our main interest in the present study has been to investigate in some detail the effects of the introduction of a ligand possessing N and O donor moieties on the photophysical and electrochemical properties of complexes **5**, **9**, and **11** in comparison to the much studied[1a] parent complex $[Ru(bpy)_3]^{2+}$ and the analogous terpyridine parent complex $[Ru(tpy)_2]^{2+}$ (**8**). A single crystal X-ray structural determination was performed for **5**, and the crystal structures of **8**, **9**, and **11** are being determined presently. Relatively few complexes containing a bipyridine moiety substituted at the 6-position have been reported.[7] We are aware of a few recent publications[8] involving complexes of the polypyridine type also containing ruthenium−oxygen bonds, but these are not photophysical studies.

Tridentate ligands offer a suitable platform for the construction of vectorially arranged donor−sensitizer−acceptor arrays. If the donor and acceptor are linked in *para*-positions to the central part of the tridentate ligands opposing each other, a linear donor−metal−acceptor axis will result. Thus, substituted terpyridines, as well as cyclometalating ligands of the dipyridylbenzene type giving organometallic complexes with Ru−N and Ru−C bonds, have been investigated as models system for electron[9] and energy[10] transfer where the donor and acceptor components have been separated by substantial intramolecular distances (10−25 Å). In studies of porphyrin triads[11] and pentads[12] which also are vectorially arranged, long-lived charge-separated states have been observed. It is of general interest to explore the photophysical properties of Ru(II) complexes based on ligands that include coordinating atoms other than nitrogen and carbon. In particular, we wanted to investigate the usefulness of novel tridentate ligands like **1** with regard to their possible use as structural elements in vectorial donor−sensitizer−acceptor arrays.

Preparations of the Complexes

The ruthenium(II) precursor $[RuCl_2(DMSO)_4]$ (**4**) is readily available from $RuCl_3 \cdot 3H_2O$ and dimethyl sulfoxide (DMSO). In our hands, the procedure by Wilkinson et al.[13] most likely yielded a mixture of *trans*- (minor) and *cis*-dichloro (major) species. Alessio et al.[14] more recently re-investigated the $[RuCl_2(DMSO)_4]$ system; and this precursor has been used in the synthesis of ruthenium(II) complexes, e.g., by Bossmann

(6) Norrby, T.; Börje, A.; Zhang, L.; Åkermark, B. *Acta Chem. Scand*., in press.

(7) (a) Della Ciana, L.; Hamachi, I.; Meyer, T. J. *J. Org. Chem.* **1989**, *54*, 1731 and references cited therein. (b) Kelly, J. M.; Long; C.; O'Connell, C. M.; Vos, J. G.; Tinnemans, A. H. A. *Inorg. Chem.* **1983**, *22*, 2818. (c) Bardwell, D. A.; Barigelletti, F.; Cleary, R. L.; Flamigni, L.; Guardigli, M.; Jeffery, J. C.; Ward, M. D. *Inorg. Chem.* **1995**, *34*, 2438. (d) Barigelletti, F.; Juris, A.; Balzani, V.; Belser, P.; von Zelewsky, A. *Inorg. Chem.* **1983**, *22*, 3335. (e) Fabian, R. H.; Klassen, D. M.; Sonntag, R. W. *Inorg. Chem.* **1980**, *19*, 1977.

(8) (a) Dovletoglou, A.; Adeyemi, S. A.; Meyer, T. J. *Inorg. Chem.* **1996**, *35*, 4120. (b) Ghatak, N.; Chakravarty, J.; Bhattacharya, S. *Transition Met. Chem. (London)* **1995**, *20*, 138. (c) Llobbet, A.; Doppelt, P.; Meyer, T. J. *Inorg. Chem.* **1988**, *27*, 514.

(9) (a) Harriman, A.; Ziessel, R. *J. Chem. Soc., Chem. Commun.* **1996**, 1707. (b) Indelli, M. T.; Scandola, F.; Collin, J.-P.; Sauvage, J.-P.; Sour, A. *Inorg. Chem.* **1996**, *35*, 303. (c) Coe, B. J.; Thompson, D. W.; Culbertson, C. T.; Schoonover, J. R.; Meyer, T. J. *Inorg. Chem.* **1995**, *34*, 3385. (d) Barigelletti, F.; Flamigni, L.; Balzani, V.; Collin, J.-P.; Sauvage, J.-P.; Sour, A.; Constable, E. C.; Cargill Thompson, A. M. W. *J. Am. Chem. Soc.* **1994**, *116*, 7692. (e) Constable, E. C.; Cargill Thompson, A. M. W.; Tocher, D. A.; Daniels, M. A. M. *New J. Chem.* **1992**, *16*, 855.

(10) (a) Grosshenny, V.; Harriman, A.; Ziessel, R. *Angew. Chem., Int. Ed. Engl*. **1995**, *34*, 1100. (b) Barigelletti, F.; Flamigni, L.; Guardigli, M.; Juris, A.; Beley, M.; Chodorowski-Kimmes, S.; Collin, J.-P.; Sauvage, J.-P. *Inorg. Chem.* **1996**, *35*, 136. (c) Chodorowski-Kimmes, S.; Beley, M.; Collin, J.-P.; Sauvage, J.-P. *Tetrahedron Lett.* **1996**, *37*, 2963. (d) Hammarström, L.; Barigelletti, F.; Flamigni, L.; Armaroli, N.; Sour, A.; Collin, J.-P.; Sauvage, J.-P. *J. Am. Chem. Soc*. **1996**, *118*, 11972.

(11) Gust, D.; Moore, T. A.; Moore, A. L.; Gao, F.; Luttrull, D.; DeGraziano, J. M.; Ma, X. C.; Makings, L. R.; Lee, S.-J.; Trier, T. T.; Bittersmann, E.; Seely, G. R.; Woodward, S.; Bensasson, R. V.; Rougée, M.; De Schryver, F. D.; Van der Auweraer, M. *J. Am. Chem. Soc.* **1991**, *113*, 3638.

(12) Gust, D.; Moore, T. A.; Moore, A. L.; Lee, S.-J.; Bittersmann, E.; Luttrull, D. K.; Rehms, A. A.; DeGraziano, J. M.; Ma, X. C.; Gao, F.; Belford, R. E.; Trier, T. T. *Science* **1991**, *248*, 199.

(13) Evans, I. P.; Spencer, A.; Wilkinson, G. *J. Chem. Soc., Dalton Trans*. **1973**, 204.

(14) (a) Alessio, E.; Mestroni, G.; Nardin, G.; Attia, W. M.; Calligaris, M.; Sava, G.; Zorzet, S. *Inorg. Chem.* **1988**, *27*, 4099. (b) Alessio, E.; Balducci, G.; Calligaris, M.; Costa, G.; Attia, W. M.; Mestroni, G. *Inorg. Chem.* **1991**, *30*, 609.

Scheme 1

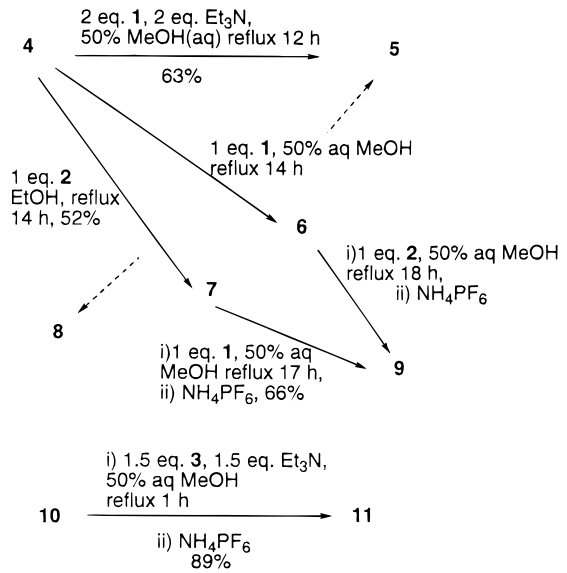

et al.[15] The homoleptic complex [Ru(6-carboxylato-bpy)$_2$] (**5**) was prepared by the reaction of 6-carboxy-bpy (**1**), triethylamine acting as a base, and **4** (Scheme 1). The intermediate **7**, [Ru(tpy)(DMSO)Cl$_2$], was prepared from **4** and tpy (**2**), which in turn was synthesized by the method of Jameson and Guise.[16] This procedure also yielded the homoleptic complex [Ru(tpy)$_2$](PF$_6$)$_2$ (**8**)[17] as a byproduct. Characterization by NMR and UV/vis yielded data for **8** which were in accordance with the literature (NMR,[9e] photophysical and electrochemical properties).[18] The heteroleptic complex [Ru(6-carboxylato-bpy)(tpy)]PF$_6$ (**9**) was obtained by the addition of 6-carboxy-bpy (**1**) to intermediate **7**. The route *via* another possible intermediate, [Ru(6-carboxylato-bpy)(DMSO)$_2$Cl] (**6**), was also explored but was found to be less suitable, overall, for the synthesis of **9**. The salt [Ru(bpy)$_2$(Pic)]PF$_6$ (**11**) (Pic = 2-carboxylatopyridine) was obtained by the reaction of 2-carboxypyridine (picolinic acid, PicH) (**3**) (Aldrich, 99%) and *cis*-[Ru(bpy)$_2$Cl$_2$]·H$_2$O (**10**), which was prepared according to Meyer et al.[19] A synthesis of the very similar compound [Ru(bpy)$_2$(Pic)]ClO$_4$, was recently reported.[8b] All species were characterized by NMR and ESI-MS.

Results

Absorption Spectra. The absorption spectra of complexes **5**, **8**, **9**, and **11** all exhibit metal-to-ligand charge-transfer (MLCT) bands in the visible region (Table 1, Figure 1), in analogy with other Ru(II)−polypyridine complexes.[1a] The coordination of carboxyl groups stabilizes the charge-transfer state (Ru(III)(acceptor ligand$^{\bullet-}$) by electron donation to Ru(III)[8a] and causes a successive red shift of this band in **9** and **11**, and even more so in **5**. The lowest ligand-centered ($\pi-\pi^*$) transitions appear around 300 nm, and in **9** this transition is split into two transitions, one from each ligand. Also notable are the bands around 350 nm present in the compounds with a coordinated carboxylate group.

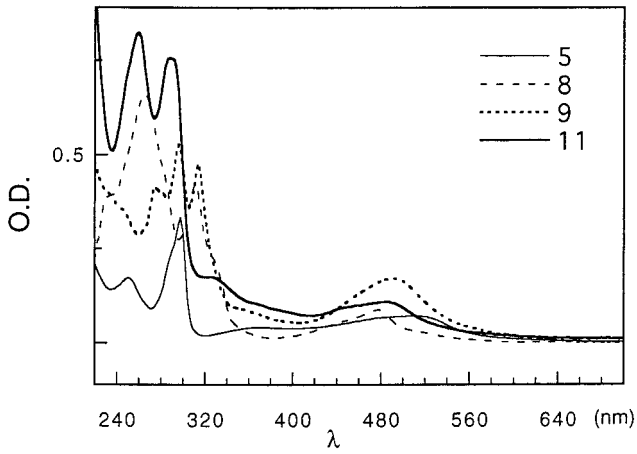

Figure 1. UV/vis spectra of [Ru(6-carboxylato-bpy)$_2$] (**5**) (1.5×10^{-5} M in EtOH/MeOH, 4:1), [Ru(tpy)$_2$](PF$_6$)$_2$ (**8**) (0.5×10^{-5} M in CH$_2$Cl$_2$/MeOH, 1:1), [Ru(6-carboxylato-bpy)(tpy)] PF$_6$ (**9**) (1.5×10^{-5} M in EtOH/MeOH, 4:1), and [Ru(bpy)$_2$(Pic)]PF$_6$ (**11**) (1×10^{-5} M in EtOH/MeOH, 4:1).

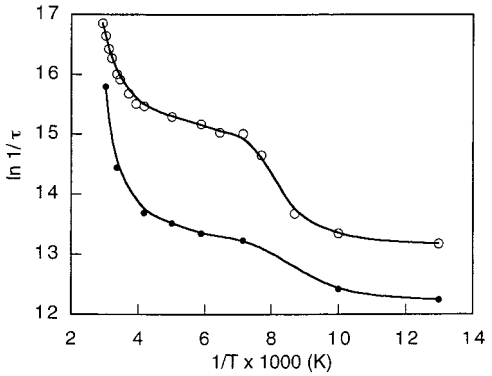

Figure 2. Temperature dependence of the rate constant for emission decay: (•) [Ru(bpy)$_3$]$^{2+}$; (○) **11**. The lines are just guides for the eye.

Emission Properties. The emission lifetime (τ) and quantum yield (Φ_{em}) were measured for the compounds in nitrogen-purged ethanol−methanol (4:1) in rigid (100 K) and fluid solvent (140 and 298 K). In rigid solvent, the emission quantum yield was high or fair for all complexes, except for **5**, and the emission lifetime was correspondingly long (Table 1). In fluid solvent, however, the lifetime and quantum yield for the complexes with tridentate ligands rapidly decreased with increasing temperature. For the complexes with bidentate ligands, [Ru(bpy)$_3$]$^{2+}$ and **11**, the emission lifetime is shown as a function of temperature in Figure 2. The quantum yield above 100 K varied in a similar manner, as expected when the rate constant for radiative deactivation, k_r, is temperature independent, since

$$\Phi_{em} = k_r\tau \qquad (1)$$

Equation 1 is valid if the emitting state is formed with unit efficiency after excitation, as is usually assumed.[20] The discontinuous change of τ and Φ_{em} around 120 K is caused by the melting of the solvent, which increases the rate constant for radiationless deactivation of the excited state.[1a] The values of k_r calculated according to eq 1 are given in Table 1.

The emission spectra for **5**, **8**, **9**, and **11** at 100 K are shown in Figure 3. On vitrification of the solvent, the emission maxima were blue-shifted and the vibrational structure became more prominent. The energies of the emission maxima were lower

(15) Bossmann, S. H.; Ghatlia, N. D.; Ottaviani, M. F.; Turro, C.; Dürr, H.; Turro, N. J. *Synthesis* **1996**, 1313.
(16) Jameson, D. L.; Guise, L. E. *Tetrahedron Lett.* **1991**, *32*, 1999.
(17) First reported by: Braddock, J. N.; Meyer, T. J. *J. Am. Chem. Soc.* **1973**, *95*, 3158.
(18) Amouyal, E.; Mouallem-Bahout, M.; Calzaferri, G. *J. Phys. Chem.* **1991**, *95*, 7641.
(19) Meyer, T. J.; Salmon, D. J.; Sullivan; B. P. *Inorg. Chem.* **1978**, *17*, 3334.
(20) Demas, J. N.; Crosby, G. A. *J. Am. Chem. Soc.* **1971**, *93*, 2841.

Table 1. Photophysical Data for the Complexes

complex	absorption data[a] (at 25 °C) λ (ϵ), nm (cm^{-1} M^{-1})		emission data[a] τ_{100K},[b] μs	τ_{140K},[b] μs	Φ_{100K}[c]	λ_{max}(100 K),[d] nm	$10^{-4}k_r$,[e] s^{-1}
9	491 (10 500)	313 (29 500) 296 (32 800)	2.76	0.24	0.073	≈675	2
5	510 (3900)	297 (18 880)	*f*	*f*	$<5 \times 10^{-4}$	≈675	*f*
8	476 (12 700)[g]	309 (54 900)	8.85	0.36	0.38	602	4.1
11	483 (9200)	292 (52 600)	1.59	0.30	0.126	644	8
$[Ru(bpy)_3]^{2+}$	450 (14 300)[h]	288 (81 000)	4.00	1.78	0.45	580	11

[a] In N_2-purged EtOH/MeOH, 4:1. [b] Emission lifetime. [c] Emission quantum yield. [d] Wavelength of maximum emission intensity (corrected). [e] Rate constant for radiative decay determined at 100 K according to eq 1. [f] Not measurable. [g] In CH_2Cl_2/MeOH, 1:1; 25 °C. [h] From: Cook, M. J.; Lewis, A. P.; McAuliffe, G. S. G.; Skarda, V.; Thomson, A. J.; Glasper, J. L.; Robbins, D. J. *J. Chem. Soc., Perkin Trans. 2* **1984**, 1293.

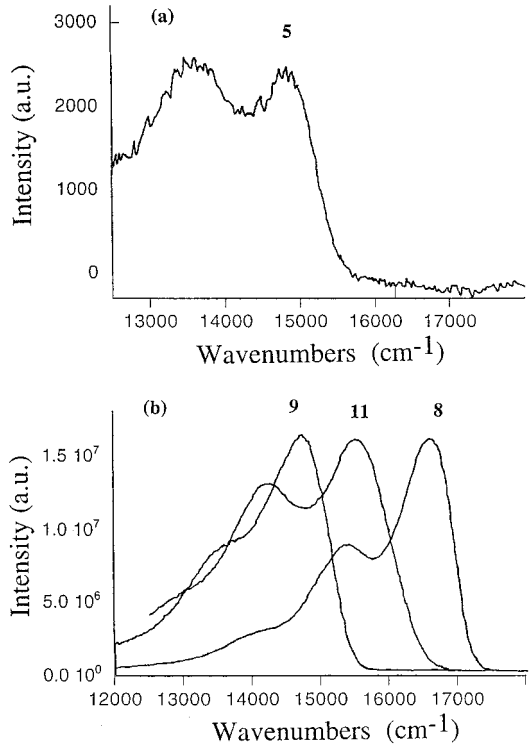

Figure 3. Corrected emission spectra at 100 K in EtOH/MeOH: (a) [Ru(6-carboxylato-bpy)$_2$] (**5**); (b) [Ru(tpy)$_2$](PF$_6$)$_2$ (**8**), [Ru(6-carboxylato-bpy)(tpy)]PF$_6$ (**9**), [Ru(bpy)$_2$(Pic)]PF$_6$ (**11**).

Table 2

complex	$E_{1/2}$(oxidn), V	$E_{1/2}$(redn), V 1	2	3
$[Ru(bpy)_3]^{2+}$	+1.31	−1.30	−1.49	−1.73
8	+1.30	−1.24	−1.49	
9	+0.90	−1.36	−1.63	
5	+0.52	−1.49	−1.79	
11	+0.88	−1.43	−1.68	≈−2.3[a]

[a] Irreversible.

for the complexes with tridentate ligands and lower when a carboxylate group was coordinated.

Electrochemical Data. The reduction potentials versus SCE for the different complexes in acetonitrile are shown in Table 2. The results for $[Ru(bpy)_3]^{2+}$ were in good agreement with previously reported values.[21] All complexes exhibited two or three reduction steps, corresponding to successive reduction of each of the ligands, and one oxidation step, corresponding to oxidation of the metal. The split in potential between the anodic and cathodic peaks for each redox step never exceeded 80 mV (scan rate 100−500 mV/s), indicating near reversibility.

(21) Tokel-Takvoryan, N. E.; Hemingway, R. E.; Bard, A. J. *J. Am. Chem. Soc.* **1973**, *95*, 6582.

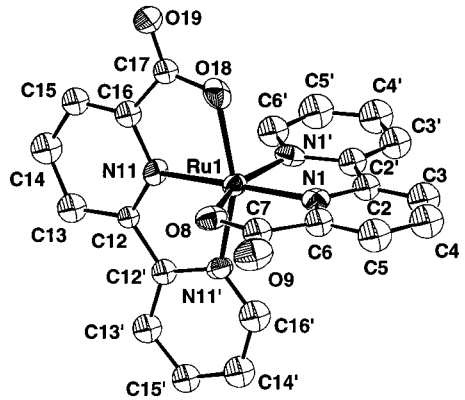

Figure 4. ORTEP plot showing one of the [Ru(6-carboxylato-bpy)$_2$] (**5**) molecules in the asymmetric unit. The ligand atoms around Ru(2) are labeled in analogy to those of Ru(1) by simply adding 20 to the numbers in the figure above. The probability ellipsoids of the atomic positions, calculated from the thermal parameters, are drawn at the 50% probability level. Hydrogen atoms are omitted.

Table 3. Fractional Atomic Coordinates ($\times 10^4$) and Thermal Parameters (U_{eq}) ($\times 10^3$) with Esd's for Selected Atoms of **5**

atom	*x*	*y*	*z*	U_{eq},[a] Å^2
Ru(1)	9883(1)	821(1)	2450(1)	29.1(4)
Ru(2)	3011(1)	2161(1)	4442(1)	34.5(5)
O(8)	9931(9)	−1037(11)	2369(3)	43(4)
O(9)	9102(9)	−2716(13)	2582(4)	50(5)
O(18)	8906(10)	1078(10)	1930(3)	40(4)
O(19)	9143(11)	1724(12)	1340(3)	57(5)
O(28)	2942(11)	338(11)	4299(3)	49(5)
O(29)	2927(13)	−1470(13)	4573(4)	70(6)
O(38)	4830(9)	2294(11)	4265(3)	42(4)
O(39)	5911(10)	2903(14)	3785(3)	63(5)
N(1)	8637(11)	310(12)	2794(3)	30(5)
N(1′)	9317(11)	2418(12)	2655(3)	31(5)
N(11)	11155(11)	1378(12)	2108(4)	33(5)
N(11′)	11343(11)	729(13)	2800(3)	36(5)
N(21)	3322(11)	1423(14)	4938(4)	33(5)
N(21′)	3216(11)	3651(14)	4780(4)	38(5)
N(31)	2773(10)	2870(13)	3941(3)	36(4)
N(31′)	1188(11)	2277(14)	4407(4)	44(5)

[a] U_{eq} is defined as one-third of the trace of the orthogonalized $\mathbf{U}_{ij}$ tensor.

Single-Crystal X-ray Diffraction Study of 5. The observed molecular structure of **5** and the atomic labeling scheme are shown in Figure 4. Fractional coordinates and equivalent isotropic temperature factors for selected atoms of **5** are given in Table 3. The unit cell of the crystal structure contains eight molecules of [Ru(6-carboxylato-bpy)$_2$] (**5**). Thus, with the space group symmetry, $P2_1/n$, there are two symmetry-independent molecules. The molecules of **5** are located in layers perpendicular to [001] separated by $c/4$. The relatively flat layers of molecules involving the Ru(1) atoms (at $z \approx \pm 1/4$) alternate with the more puckered molecular layers involving the Ru(2) atoms (at $z \approx 0, 1/2$). Two slightly disordered ethanol molecules

occupy the void formed between the layers of **5**. (For the unit cell packing diagram, see Supporting Information Figure S6.) The ruthenium atoms are six-coordinated by four nitrogen and two oxygen atoms: two nitrogen atoms and one of the carboxylate oxygen atoms from each of the two ligand molecules **1**. The angles between the planes of the two ligands **1** within the complex are 87.8(3) and 86.0(3)° for the two independent molecules.

Discussion

Redox and Photophysical Properties. (a) Redox Properties and the Nature of the Lowest Excited State. In **9** and **11**, the coordinated carboxylate decreases the $Ru^{II/III}$ reduction potential by ≈0.4 V and the potentials for the ligand-based reductions are decreased by ≈0.12 V (Table 2). The shifts may be explained by (i) a higher electron density on the metal, (ii) a lower overall charge of the complex that stabilizes the oxidized species of each redox couple due to a smaller difference in solvation energy, and (iii) a Coulombic repulsion between the additional (negative) charge of the carboxylate and the electrons on the reduced ligands that causes a negative shift of the potentials of the ligand-based reductions. The much larger shift in the $Ru^{II/III}$ potential compared to the potential for ligand reduction indicates that the increased electron density on the metal is the most important contribution. When yet another carboxylate is coordinated in **5**, the $Ru^{II/III}$ potential is decreased by an additional 0.4 V; i.e., there is a linear dependence of this potential on the number of coordinated carboxylate groups in the series **8**−**9**−**5**.

The lowest excited state of $[Ru(bpy)_3]^{2+}$, $[Ru(tpy)_2]^{2+}$ (**8**), and their derivatives is a closely spaced manifold of ^{3}MLCT states.[1a,3a,c,d,22] The MLCT state of each complex is localized on the ligand having the lowest π^* energy level and thus is the easiest to reduce. It has been shown that the energy of the emission (and absorption to the lowest singlet MLCT state) depends linearly on the difference between the reduction potentials for the first oxidation (metal-based $Ru^{II/III}$) and the first reduction (ligand-based), $\Delta E_{1/2}$, as determined electrochemically.[23] This supports the model of the lowest excited state as a MLCT state localized on one ligand.

The complexes **9** and **11** are heteroleptic, and thus there may be MLCT states involving different ligands. In **11**, only two reversible ligand reductions were observed, and they were attributed to bpy reductions. The reduction observed around −2.3 V (vs SCE) was highly irreversible and resulted in oxidative peaks around −0.7 V upon scan reversal, and is attributed to a further reduction of an already reduced bipyridine (*cf.* $[Ru(bpy)_3]^{2+}$).[21] Since no reduction of the 2-carboxylatopyridine was seen in the ground state, the lowest excited MLCT state would thus be bpy-based. In **9**, it is not clear which ligand is the first to be reduced electrochemically; the potentials for both reduction processes are shifted in parallel fashion in the series **8**−**9**−**5**. However, a comparison of the emission spectra at 100 K (Figure 3b) shows that those of **8** and **9** exhibit the same, relatively narrow shape, while that of **11** is broader, with a higher relative intensity of the second vibrational peak, similar to the spectrum of $[Ru(bpy)_3]^{2+}$.[24] Therefore, we believe that the lowest MLCT state of **9** is terpyridine-based.[25] In Figure 5, the energies of the maxima in the absorption (lowest MLCT band) and low-temperature emission are plotted as a function of $\Delta E_{1/2}$ (*vide supra*). The dependencies are linear (except for the emission of **5**), although the slopes are not unity.[23] According to Figure 5, the emission maximum for **5** would be expected to lie around 775 nm instead of 675 nm, as is observed (a difference corresponding to 0.25 eV). This unexpectedly high value of the excited state energy would imply that **5** is a very strong excited state reductant,[26] ≈−1.3 V vs SCE compared to −0.85 V for $[Ru(bpy)_3]^{2+}$.[1a] However, the observed quantum yield for **5** is extremely low, considering the low temperature, and it is possible that the observed emission instead originates from an emitting impurity and that **5** is nonemitting also at this temperature.

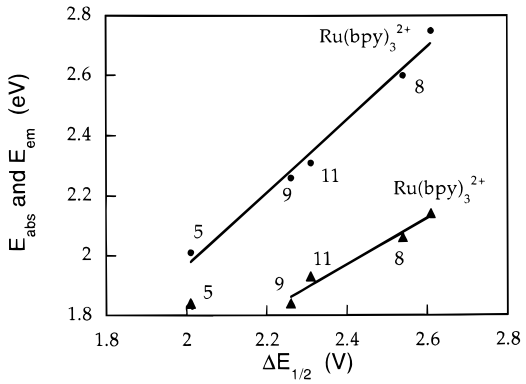

Figure 5. Energies of the maxima in the absorption (•) and emission (▲) spectra as a function of $\Delta E_{1/2}$. $\Delta E_{1/2}$ is the difference between the reduction potentials for the $Ru^{II/III}$ oxidation and the first ligand reduction.

(b) Excited State Lifetime. It is generally agreed that the drastic decrease in the excited-state lifetime of Ru(II) polypyridine complexes observed at higher temperatures may be ascribed to rapid deactivation via thermally populated metal-centered (MC) states.[1a,3] Although the activation energy (ΔE_1) for population of the MC states is high (see eq 2), the transition frequency factor is high and the MC state lifetime is short, so they contribute to a major part of the total deactivation as the temperature is increased. In the bidentate $[Ru(bpy)_3]^{2+}$, ΔE_1 ≈ 3600 cm^{-1}.[1a,9c] In $[Ru(tpy)_2]^{2+}$ (**8**), the situation is different. The tpy ligand is not strictly planar, and the Ru−N bond distance is shorter for the central pyridine than for the terminal rings. Therefore, the tpy ligands are not quite compatible with an octahedral geometry. The ligand field splitting (10*Dq*) is reduced,[9a,27] which leads to a smaller energy difference between the MCLT and MC states and a smaller value of ΔE_1 (≈1500 cm^{-1}).[28] Also in Ru(II) complexes with bidentate ligands, the value of ΔE_1 is reduced when substituents are introduced on the ligands which distort the geometry by purely steric interactions.[7b−e,24]

In **9**, the emission lifetime and quantum yield at 100 and 140 K are comparable with those of $[Ru(tpy)_2]^{2+}$ (**8**). Thus, the introduction of a coordinated carboxylate group does not

(22) Rillema, D. P.; Blanton, C. B.; Shaver, R. J.; Jackman, D. C.; Boldaji, M.; Bundy, S.; Worl, L. A.; Meyer, T. J. *Inorg. Chem.* **1992**, *31*, 1600.
(23) (a) Dodsworth, E. S.; Lever, A. B. P. *Chem. Phys. Lett.* **1985**, *119*, 61. (b) Dodsworth, E. S.; Lever, A. B. P. *Chem. Phys. Lett.* **1986**, *124*, 152.
(24) Hammarström, L.; Alsins, J.; Börje, A.; Norrby, T.; Zhang L.; Åkermark, B. *Photochem. Photobiol A* **1997**, *102*, 139.
(25) Maestri, M.; Armaroli, N.; Balzani, V.; Constable, E. C.; Cargill Thompson, A. M. W. *Inorg. Chem.* **1995**, *34*, 2759.
(26) The reduction potential $E^{Ru(*II/III)}$ of the excited state was calculated from $E^{Ru(*II/III)} = E^{Ru(II/III)} - E_{em}$, where $E^{Ru(II/III)}$ is the corresponding ground-state potential and E_{em} is the 0−0 emission energy, estimated from the maximum in the spectrum in rigid solvent. In this estimate, the usual assumption is made of a negligible entropy difference between the ground and excited states.
(27) Constable, E. C.; Cargill Thompson, A. M. W.; Armaroli, N.; Balzani, V.; Maestri, M. *Polyhedron* **1992**, *11*, 2707.
(28) Hecker, C. R.; Gushurst, A. K. I.; McMillin, D. R. *Inorg. Chem.* **1991**, *30*, 538.

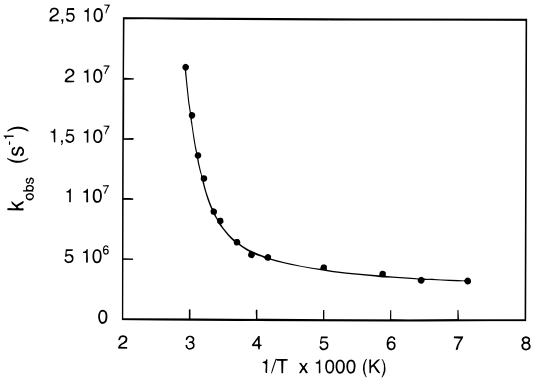

Figure 6. Temperature dependence of the rate constant for emission decay in the fluid-solvent region for $[Ru(bpy)_2(Pic)]PF_6$ (**11**). The line is a least-squares fit to eq 2.

necessarily result in complexes with poor emission properties at low temperature. On the contrary, in **11**, the emission lifetime (120 ns) and quantum yield (0.01) are rather high also at room temperature. A fit of the lifetime data for **11** in the fluid-solvent region (Figure 6) was made to the equation

$$1/\tau = k_0 + A_1 \exp(-\Delta E_1/RT) + A_2 \exp(-\Delta E_2/RT) \quad (2)$$

where k_0 is the low-temperature value, ΔE_1 is the activation energy for population of MC states (*vide supra*), and the second exponential term is needed to account for the temperature-dependent population distribution between the different states in the lowest MLCT manifold.[1a] The values obtained were $A_1 = 1.3 \times 10^{12}$ s^{-1} and $\Delta E_1 = 2700$ cm^{-1}. It would have been desirable to extend the range of data points, especially to higher temperatures, but the weak emission already at 343 K prevented any further extension of the range. Although the fit was good (Figure 6), these values must therefore be taken with some caution. However, it is clear that Ru(II) complexes with coordinated carboxylate groups may be synthesized that exhibit fairly good emission properties as demonstrated by the emission lifetime of 120 ns for **11** at 298 K. The higher value of ΔE_1 compared to that for $[Ru(tpy)_2]^{2+}$ (**8**) is expected to be due to a smaller distortion from the approximately octahedral coordination geometry of the parent compound $[Ru(bpy)_3]^{2+}$ than in the complexes with tridentate ligands.

At temperatures below 240 K, the energy gap law may explain most of the reduction of the excited state lifetime of **11** compared to that of $[Ru(bpy)_3]^{2+}$.[27c,29] At 100 K, the first exponential term in eq 2 is negligible, and the radiationless deactivation of the excited state occurs only directly to the ground state, with a rate constant k_{nr}. The value of k_{nr} is given by $k_{obs} = k_{nr} + k_r$, where $k_{obs} = 1/\tau$ and k_r is calculated from eq 1. With the emission energy, E_{em}, given by the energy of the emission maximum, we obtain $\Delta \ln(k_{nr})/\Delta E_{em} = -8.1 \times 10^{-4}$ cm at 100 K, for the **11**$-[Ru(bpy)_3]^{2+}$ couple, where $\Delta \ln(k_{nr})$ and ΔE_{em} denote the difference in properties between the two complexes. This value is similar to those reported by Meyer et al.[29a] in their investigations of the energy gap law for different polypyridine complexes of Ru(II) and Os(II). At higher temperatures, up to 240 K, we obtain similar values. An analysis as above of the differences between the photophysics of the terpyridine-based chromophores **8** and **9** is difficult, since meaningful data for **9** were not obtainable much above 140 K.

Table 4. Selected Bond Distances (Å) and Angles (deg) with Esd's for **5**

(a) Distances

molecule 1		molecule 2	
Ru(1)−O(8)	2.106(12)	Ru(2)−O(28)	2.109(12)
Ru(1)−O(18)	2.129(11)	Ru(2)−O(38)	2.132(10)
Ru(1)−N(1)	1.949(12)	Ru(2)−N(21)	1.958(14)
Ru(1)−N(1′)	2.037(13)	Ru(2)−N(21′)	2.061(15)
Ru(1)−N(11)	1.979(13)	Ru(2)−N(31)	1.952(11)
Ru(1)−N(11′)	2.015(12)	Ru(2)−N(31′)	2.026(12)
O(8)−C(7)	1.31(2)	O(28)−C(27)	1.30(2)
O(9)−C(7)	1.21(2)	O(29)−C(27)	1.23(3)
O(18)−C(17)	1.28(2)	O(38)−C(37)	1.29(2)
O(19)−C(17)	1.23(2)	O(39)−C(37)	1.25(2)

(b) Angles

molecule 1		molecule 2	
O(8)−Ru(1)−O(18)	91.8(4)	O(28)−Ru(2)−O(38)	91.5(5)
O(8)−Ru(1)−N(1)	79.2(5)	O(28)−Ru(2)−N(21)	78.9(5)
O(8)−Ru(1)−N(1′)	158.2(4)	O(28)−Ru(2)−N(21′)	158.2(5)
O(8)−Ru(1)−N(11)	102.1(5)	O(28)−Ru(2)−N(31)	100.1(5)
O(8)−Ru(1)−N(11′)	90.5(5)	O(28)−Ru(2)−N(31′)	91.0(6)
O(18)−Ru(1)−N(1)	103.0(5)	O(38)−Ru(2)−N(21)	98.3(5)
O(18)−Ru(1)−N(1′)	91.8(4)	O(38)−Ru(2)−N(21′)	91.2(5)
O(18)−Ru(1)−N(11)	77.7(5)	O(38)−Ru(2)−N(31)	79.2(4)
O(18)−Ru(1)−N(11′)	157.0(4)	O(38)−Ru(2)−N(31′)	158.0(5)
N(1)−Ru(1)−N(1′)	79.0(5)	N(21)−Ru(2)−N(21′)	79.3(6)
N(1)−Ru(1)−N(11)	178.5(5)	N(21)−Ru(2)−N(31)	177.4(5)
N(1)−Ru(1)−N(11′)	100.0(5)	N(21)−Ru(2)−N(31′)	103.6(5)
N(1′)−Ru(1)−N(11)	99.7(5)	N(21′)−Ru(2)−N(31)	101.7(6)
N(1′)−Ru(1)−N(11′)	94.5(5)	N(21′)−Ru(2)−N(31′)	94.5(6)
N(11)−Ru(1)−N(11′)	79.4(5)	N(31)−Ru(2)−N(31′)	78.8(5)
Ru(1)−O(8)−C(7)	114.4(10)	Ru(2)−O(28)−C(27)	114.2(12)
Ru(1)−O(18)−C(17)	113.9(10)	Ru(2)−O(38)−C(37)	112.5(10)

Thus, the value of ΔE_1 for **9** is not known, although the fact that the emission above 140 K was relatively weak in itself suggests an increased deactivation via MC states for **9** compared to **8**. However, at 100 K, one may note that the value of $\Delta \ln(k_{nr})/\Delta E_{em} = -8.6 \times 10^{-4}$ cm for the **8**$-$**9** couple, indicating that, also for these terpyridine complexes, most of the difference in lifetimes can be ascribed to the energy gap law at this temperature.

Single-Crystal X-ray Diffraction Study of 5. Selected bond lengths and bond angles are given in Table 4. Due to the constraints imposed by the geometry of the ligand molecules, most of the N−Ru−N and the O−Ru−N bond angles deviate significantly from the ideal values for an octahedral coordination geometry. Thus, the coordination around the ruthenium atoms can only approximately be regarded as octahedral, similar to the structures found for **8** and **9**.[30] The ruthenium−nitrogen distances to the central nitrogen atoms of the carboxylato-substituted pyridine ring (unprimed atomic labels) are generally smaller (1.95−1.98 Å) than those to the nitrogen atoms of the unsubstituted pyridine ring (primed atom labels) (2.01−2.04 Å) (Table 4a). The bond lengths for the latter agree with those previously published for $[Ru(bpy)_3](PF_6)_2$.[31] The bond lengths within the ligand molecules are generally slightly shorter than those found in bpy itself. This shortening is probably related to the rather large thermal vibrations of the ligand molecules. Most of the deviations of the intramolecular bond angles can be ascribed to substituent effects.[32] The carbon−oxygen distances in the carboxylato groups are, as expected, longer (1.28−1.31 Å) between the carbonyl carbon and the oxygen

(29) (a) Lumpkin, R. S.; Meyer, T. J. *J. Phys. Chem.* **1986**, *90*, 5307. (b) Treadway, J. A.; Loeb, B.; Lopez, R.; Anderson, P. A.; Keene, F. R.; Meyer, T. J. *Inorg. Chem.* **1996**, *35*, 2242. (c) Caspar, J. V.; Kober, E. M.; Sullivan, B. P.; Meyer, T. J. *J. Am. Chem. Soc.* **1982**, *104*, 630.

(30) Lashgari, K.; Norrestam, R. Manuscript in preparation.

(31) Rillema, D. P.; Jones, D. S.; Woods, C.; Levy, H. A. *Inorg. Chem.* **1992**, *31*, 2935.

(32) (a) Norrestam, R.; Schepper, L. *Acta Chem. Scand.* **1978**, *A32*, 889. (b) Norrestam, R.; Schepper, L. *Acta Chem. Scand.* **1981**, *A35*, 91.

atom involved in the ruthenium coordination than (1.21−1.25 Å) the free carbonyl oxygen atom distances. Superposing the two symmetry-independent molecules of **5** by least-squares techniques, using the method described by Diamond,[33] shows that these molecules have very similar conformations. Thus, the largest deviation between related atoms in the two molecules is 0.43 Å with a root-mean-square deviation of only 0.17 Å.

Conclusion

In this work, we have investigated the photophysical and electrochemical properties of a series of ruthenium complexes displaying Ru−N and Ru−O bonds. A general correlation of the electrochemical properties and the number of carboxylate groups per complex has been found, ca. 0.4 V lower reduction potential for the oxidation step (Ru(II/III)) per carboxylate group. To the best of our knowledge, this is the first report of luminescent mononuclear Ru(II) complexes containing pyridinecarboxylate ligands (**9** and **11**), and the emission lifetime of **11** is as long as 120 ns at room temperature. This has implications for the further development of photoelectron transfer catalyst candidates: tridentate building blocks for vectorial arrays based on **1** with useful emission properties likely could be developed. A large difference was noted between the emission properties of **5**, which practically lacks emission, and the other complexes **8**, **9**, and **11** which have emission at low temperatures 100−140 K (**11** at even higher temperatures). Nonradiative deactivation pathways involving low-lying MC-dd are commonly invoked for bipyridine[3,27c] and terpyridine[9d,e] complexes, many of which display a drastic decrease of the excited state lifetime at higher temperatures. This kind of temperature dependence is seen clearly in **11** and $[Ru(bpy)_3]^{2+}$ and more drastically in **8** and **9**. The structure of **5** as determined by single-crystal X-ray diffraction is quite interesting, with a rather small equatorial distortion. The larger deviations, from the ideal 180° in a true octahedron, of the N−Ru−O bonds (ca. 158°) in the axial plane are apparently due to constraints imposed by the ligand geometry. We have not been able to correlate the photophysical properties of the complexes in this study in any simple way to the varying degree and character of the geometrical distortion of the coordination polyhedron. Further studies of such possible correlations are being pursued by 2D NMR and X-ray crystallographic methods.[30]

Experimental Section

Methods. The ^{1}H NMR and ^{13}C NMR spectra of complexes **4**−**11** were recorded in deuterated chloroform, methanol, DMSO, or acetone on Bruker AM 400 (400 MHz proton, 100 MHz carbon) and DMX 500 (500 MHz proton, 125 MHz carbon) instruments. Chemical shifts (δ) are reported in parts per million (ppm) downfield from TMS (tetramethylsilane). Assignment of the ^{1}H and ^{13}C resonances was supported by 2D NMR techniques. Analytical TLC was performed on precoated aluminum oxide gel 60 F_{254} plates (Al_2O_3, neutral, Merck) with UV detection. Aluminum oxide gel (Al_2O_3, neutral, Brockmann I, 150 mesh, Aldrich) was used for preparative column chromatography. The electronic absorption spectra were recorded on a Varian Cary 5E UV/vis/NIR spectrophotometer at 25.0 °C (±0.1 °C). The electrospray ionization mass spectrometry (ESI-MS) experiments were performed on a ZabSpec mass spectrometer (VG Analytical, Fisons instrument). Electrospray conditions: needle potential, 3 kV; acceleration voltage, 4 kV; bath and nebulizing gas, nitrogen. Liquid flow was 50 μL/min using a syringe pump (Phoenix 20, Carlo Erba, Fisons instrument). Solvent composition was 50% acetonitrile−50% water containing 1% acetic acid. Accurate mass measurements were obtained by the use of poly(ethylene glycol) (PEG) as an internal standard.

(33) Diamond, R. *Acta Crystallogr.* **1988**, *A44*, 2.

Materials. Diethyl ether (ether), ethyl acetate (EtOAc), and dichloromethane (CH_2Cl_2) were distilled prior to use (Kebo AB, grade purum). Deionized water was used in all experiments. Methanol and dimethyl sulfoxide (DMSO) of 99+% HPLC grade (Aldrich), acetic acid (HOAc) (99.8%, Aldrich), ethanol (99.5%, spectroscopic grade, Kemetyl), 2,2′-bipyridine (99%, pro analysi, Aldrich), 2-carboxypyridine (**3**) (99%, Aldrich), $RuCl_3 \cdot 3H_2O$ (41.71% Ru assay, Aldrich,), triethylamine (99%, pro synthesis, Merck), and NH_4PF_6 (95+%, Aldrich) were used as received. 6-carboxy-bpy (**1**)[6] and $[Ru(bpy)_3]^{2+}$ were available from earlier studies; $[RuCl_2(DMSO)_4]$ (**4**),[13] *cis*-$[Ru(bpy)_2Cl_2] \cdot H_2O$ (**7**),[19] and 2,2′:6′,2″-terpyridine (**2**)[16] were prepared according to the literature procedures cited.

Analyses. The analyses (carbon, hydrogen, and nitrogen; reported in mass %) were performed by Analytische Laboratorien GmbH, D-51789 Lindlar, Germany.

Syntheses. (a) Bis(6-carboxy-2,2′-bipyridinato)ruthenium(II), [Ru(6-carboxylato-bpy)$_2$] (5). $[RuCl_2(DMSO)_4]$ (**4**) (55 mg, 0.113 mmol) and 6-carboxy-bpy (**1**) (45.5 mg, 0.227 mmol) were dissolved in 50% aqueous MeOH (MeOH, 99+%, 10 mL, and deionized water, 10 mL), and the solution was degassed by pumping and flushing with argon on the vacuum line. Triethylamine (32 μL, 23 mg, 0.227 mmol) was added, and the mixture was refluxed under argon overnight (12 h). TLC on the reaction mixture (eluent CH_2Cl_2/MeOH, 9:1) showed one intensely purple main product ($R_f \approx 0.89$). Most of the solvents were evaporated on a rotary evaporator, and crude **5** was obtained (101 mg, containing some DMSO and triethylammonium chloride). This mixture was dissolved in CH_2Cl_2/MeOH together with Al_2O_3 (0.9 g), the solution was again evaporated on the rotary evaporator, and the residue was dried at the pump overnight. The Al_2O_3 gel containing **5** was put on top of a column of Al_2O_3 (100 mL dry volume, height 17 cm, diameter 3 cm, neutral, 150 mesh, Merck, slurry-packed in CH_2Cl_2) and eluted with 300 mL of eluent (CH_2Cl_2/MeOH, 9:1), which yielded the main fraction (36 mg, 0.07 mmol, 62%). At the end of the chromatography, addition of 50 mL of MeOH gave a minor fraction of [Ru(6-carboxylato-bpy)$(DMSO)_2$Cl] (**6**) (*vide infra*). Recrystallization by slow diffusion of ether into an ethanolic (99.5%) solution of **5** yielded X-ray-quality crystals.

UV/vis: λ_{max} 297 nm (ϵ = 18 800 M^{-1} cm^{-1}), 510 nm (ϵ = 3 900 M^{-1} cm^{-1}) in EtOH/MeOH (4:1). ESI-MS, *m*/*z*: found for $[M + H]^+$, 500.991; simulated monoisotopic mass for $C_{22}H_{15}N_4O_4Ru$, 501.014. Several acetonitrile and water adducts were observed. For spectra, see SI (Supporting Information) Figure S1. ^{1}H NMR (400 MHz, $CDCl_3$/MeOH-d_4 (1:1), $CDCl_3$ peak at 7.56 ppm), δ: 8.63 (dd, J = 1.0, 8.2 Hz, 2 H, H-3); 8.37 (ddd, J = 0.9, 1.2, 8.1 Hz, 2 H, H-3′); 8.30 (dd, J = 1.0, 7.6 Hz, 2 H, H-5); 8.10 (dd, J = 7.6, 8.2 Hz, 2 H, H-4); 7.72 (ddd, J = 2.1, 5.7, 7.0 Hz, 2 H, H-4′); 7.10 (ddd, J = 1.2, 5.7, 7.0 Hz, 2 H, H-5′); 7.07 (ddd, J = 0.9, 2.1, 5.7 Hz, 1 H, H-6′). ^{13}C NMR (100 MHz, $CDCl_3$/MeOH-d_4 (1:1 v/v), middle $CDCl_3$ peak at 78.7 ppm), δ: 174.8, 160.8, 157.1, 154.1 (C-6′), 154.1, 136.6 (C-4′), 134.5 (C-4), 127.8 (C-5′), 127.1 (C-5), 125.2 (C-3), 124.2 (C-3′).

(b) Dichloro(2,2′:6′,2″-terpyridine)(dimethyl sulfoxide)ruthenium-(II), [Ru(tpy)(DMSO)Cl$_2$] (7). $[RuCl_2(DMSO)_4]$ (**4**) (415 mg, 0.857 mmol, 1.0 equiv) was dissolved in a mixture of EtOH (8 mL, 99.5%) and MeOH (2 mL, 99.5%), degassed by pumping and flushing with argon on the vacuum line, and the mixture was refluxed for 15 min. A solution of tpy (**2**) (197 mg, 0.844 mmol, 0.98 equiv) in EtOH (2 mL, 99.5%) was added dropwise over 25 min to the refluxing solution of **4**. The reaction solution gradually became a dark brown, thick slurry, while being refluxed for another 12 h. The mixture was allowed to cool, and **7** settled out as a precipitate, which was filtered off and washed with several aliquots of water, followed by cold EtOH, until the washings were clear. The solid **7** was dried at the pump (213 mg, 0.441 mmol, 52%).

UV/vis: λ_{max} 481 nm (ϵ = 4100 M^{-1} cm^{-1}) in CH_2Cl_2/MeOH (9:1). ESI-MS, *m*/*z*: found for $[M - Cl + CH_3CN]^+$, 488.942; simulated monoisotopic mass for $C_{19}H_{20}N_4OSClRu$, 489.009. For spectra, see SI Figure S2. ^{1}H NMR (400 MHz, DMSO-d_6), δ: 9.03 (ddd, J = 0.8, 1.7, 5.5 Hz, 2 H, H-6 and H-6″); 8.58 (ddd, J = 0.7, 1.4, 8.1 Hz, 2 H, H-3 and H-3″); 8.53 (d, J = 7.9 Hz, 2 H, H-3′ and H-5′); 8.15 (dt J = 1.5, 7.9 Hz, 2 H, H-4 and H-4″); 8.03 (t, J = 8.1 Hz, 1 H, H-4′); 7.79

(ddd, J = 1.5, 5.5, 7.6 Hz, 2 H, H-5 and H-5″). The DMSO was exchanged with the solvent DMSO-d_6 molecules and was thus not observed.

(c) Bis(2,2′:6′,2″-terpyridine)ruthenium(II) Bis(hexafluorophosphate), [Ru(tpy)$_2$](PF$_6$)$_2$ (8). Compound **8** was sometimes obtained as a byproduct during the synthesis of **7** and was isolated by the addition of concentrated aqueous NH_4PF_6 to the bright red solution phase remaining after the sedimentation of **7** (*vide supra*). Analytical data conformed to those expected. For ESI-MS spectra, see SI Figure S3.

(d) (6-Carboxy-2,2′-bipyridinato)(2,2′:6′,2″-terpyridine)ruthenium(II) Hexafluorophosphate, [Ru(6-carboxylato-bpy)(tpy)]PF$_6$ (9). [Ru(tpy)(DMSO)Cl$_2$] (**7**) (100 mg, 0.2 mmol) and 6-carboxy-bpy (**1**) (40 mg, 0.2 mmol) were dissolved in 50% aqueous MeOH (MeOH, 99+%, 10 mL, and deionized water, 10 mL), and the solution was degassed by pumping and flushing with argon on the vacuum line. Triethylamine (28 μL, 20.2 mg, 0.2 mmol) was added, and the resulting solution turned strongly reddish-yellow and became rapidly darker upon heating. Refluxing was maintained under argon for 17 h. The mixture was allowed to cool and then filtered through a glass frit (P3). Aqueous NH_4PF_6 was added, resulting in the crystallizaation of **9**, which was collected, washed with water, and dried at the pump (89.3 mg, 0.131 mmol, 66%).

UV/vis: λ_{max} 296 nm (ϵ = 32 800 M^{-1} cm^{-1}), 313 nm (ϵ = 29 500 M^{-1} cm^{-1}), 491 nm (ϵ = 10 500 M^{-1} cm^{-1}) in EtOH/MeOH (4:1). ESI-MS, *m*/*z*: found for [M]$^+$, 534.041; simulated monoisotopic mass for $C_{22}H_{15}N_4O_4Ru$, 534.050. For spectra, see SI Figure S4. ^{1}H NMR (400 MHz, acetone-d_6), δ: 9.02 (dd, J = 1.2, 8.0 Hz, 1 H, H-3 bpy); 8.91 (d, J = 8.2 Hz, 2 H, H-3′ and H-5′ tpy); 8.73 (ddd, J = 0.8, 1.3, 8.1 Hz, 2 H, H-3 and H-3″ tpy); 8.72 (ddd, J = 0.9, 1.5, 7.9 Hz, 1 H, H-3′ bpy); 8.45 (dd, J = 7.6, 8.0 Hz, 1 H, H-4 bpy); 8.37 (dd, J = 1.2, 8.0 Hz, 1 H, H-5 bpy); 8.30 (t, J = 8.2 Hz, 1 H, H-4′ tpy); 8.04 (ddd, J = 1.5, 7.5, 8.1 Hz, 2 H, H-4 and H-4″ tpy); 7.91 (ddd, J = 1.5, 7.6, 7.9 Hz, 1 H, H-4′ bpy); 7.64 (ddd, J = 0.8, 1.5, 5.6 Hz, 2 H, H-6 and H-6″ tpy); 7.42 (ddd, J = 1.3, 5.6, 7.5 Hz, 2 H, H-5 and H-5″ tpy); 7.39 (ddd, J = 0.9, 1.5, 5.7 Hz, 1 H, H-6′ bpy); 7.15 (ddd, J = 1.5, 5.7, 7.6 Hz, 1 H, H-5′ bpy). ^{13}C NMR (100 MHz carbon, acetone-d_6), δ: 171.6 (carbonyl), 159.7, 159.1, 157.0, 155.6, 154.4 (C-6 bpy), 153.5, 152.4 (C-6 and C-6″ tpy), 138.0 (C-4 and C-4″ tpy), 137.2 (C-4 bpy), 136.0 (C-4′ bpy), 134.2 (C-4′ tpy), 128.2 (C-5 and C-5″ tpy), 127.6 (C-5′ bpy), 126.7 (C-5′ bpy), 125.5 (C-3′ bpy), 124.6 (C-4 bpy), 124.4 (C-3 and C-3″ tpy), 123.6 (C-3′ and C-5′ tpy).

(e) (2-Carboxypyridinato)bis(2,2′-bipyridine)ruthenium(II) Hexafluorophosphate, [Ru(bpy)$_2$(Pic)]PF$_6$ (11). A solution of *cis*-[Ru(bpy)$_2$Cl$_2$]·H$_2$O (**7**) (0.100 g, 0.19 mmol), 2-carboxypyridine (PicH) (**3**) (0.035 g, 0.29 mmol), and triethylamine (0.029 g, 40 μL, 0.29 mmol) was refluxed in 50% aqueous MeOH (MeOH, 99%, 7.5 mL, and deionized water, 7.5 mL) under argon for 1 h, at which point the reaction was complete according to TLC ($R_f \approx$ 0.68, eluent EtOAc/MeOH/HOAc/water, 15:5:1:1). To the warm, deep red solution was added NH_4PF_6 (0.085 g, 0.52 mmol) in 1 mL of water. The solution was left to cool overnight under argon. Some of the methanol was removed on the rotary evaporator, and precipitation ensued. After 5 h, the precipitate was filtered off, washed with cold water and then ether, and dried *in vacuo* at the pump. Dark red crystals of **11** (0.113 g, 0.17 mmol, 89%) were obtained. Analy. Calcd for $C_{26}H_{20}N_5O_2RuPF_6$: C, 45.89; H, 2.96; N, 10.29. Found: C, 45.74; H, 3.03; N, 10.44.

UV/vis: λ_{max} 292 nm (ϵ = 52 600 M^{-1} cm^{-1}), 483 nm (ϵ = 9200 M^{-1} cm^{-1}) in EtOH/MeOH (4:1), lit.[8b] 500 nm (ϵ = 10 100 M^{-1} cm^{-1}) in CH_3CN. ESI-MS, *m*/*z*: found for [M]$^+$, 536.035; simulated monoisotopic mass for $C_{26}H_{20}N_5O_2Ru$, 536.067. For spectra, see SI Figure S5. For a guide to the assignment of the protons, see Figure 7. ^{1}H NMR (500 MHz, acetone-d_6/MeOH-d_4, 1:1) data are as follows. bpy-1 (rings A and X), δ: 8.84 (ddd, J = 0.8, 1.4, 5.6 Hz, 1 H, H-6a); 8.69 (ddd, J = 0.9, 1.2, 8.3 Hz, 1 H, H-3a); 8.63 (ddd, J = 0.8, 1.5, 8.1 Hz, 1 H, H-3x); 8.15 (ddd, J = 1.5, 7.6, 8.1 Hz, 1 H, H-4a); 7.99 (ddd, J = 0.8, 1.5, 5.7 Hz, 1 H, H-6x); 7.96 (ddd, J = 1.5, 7.6, 8.1 Hz, 1 H, H-4x); 7.76 (ddd, J = 1.3, 5.6, 7.6 Hz, 1 H, H-5a); 7.35 (ddd, J = 1.3, 5.7, 7.5 Hz, 1 H, H-5x). bpy-2 (rings B and Y), δ: 8.71 (ddd, J = 0.8, 1.3, 8.3 Hz, 1 H, H-3b); 8.62 (ddd, J = 0.9, 1.4, 8.1 Hz, 1 H, H-3y); 8.14 (ddd, J = 1.5, 7.6, 8.2 Hz, 1 H, H-4b); 8.06 (ddd, J = 0.8, 1.5, 5.6 Hz, 1 H, H-6b); 7.97 (ddd, J = 1.5, 7.6, 8.1 Hz, 1 H, H-4y); 7.75 (ddd, J = 0.8, 1.4, 5.6 Hz, 1 H, H-6y); 7.59 (ddd, J = 1.3, 5.6, 7.6 Hz, 1 H, H-5b); 7.33 (ddd, J = 1.2, 5.7, 7.6 Hz, 1 H, H-5y). 2-Carboxylatopyridine (ring C), δ: 8.11 (ddd, J = 0.8, 1.6, 7.8 Hz, 1 H, H-3c); 8.00 (dt, J = 1.5, 7.7 Hz, 1 H, H-4c); 7.68 (ddd, J = 0.8, 1.6, 5.6 Hz, 1 H, H-6c); 7.47 (ddd, J = 1.6, 5.5, 7.7 Hz, 1 H, H-5c). ^{13}C NMR (125 MHz carbon, acetone-d_6/MeOH-d_4, 1:1), δ: 173.5, 159.5, 158.4, 158.0, 153.6, 153.5, 152.2, 151.5, 151.0, 150.7, 137.8, 137.3, 136.9, 136.1, 129.1, 127.6, 127.2, 126.8, 124.4, 124.0, 123.7. An independent report of the synthesis of the corresponding perchlorate salt was recently published.[8b]

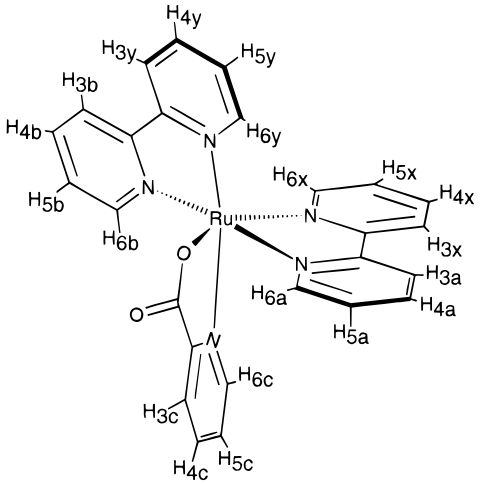

Figure 7. Labeling of the protons used in the NMR assignment of **11**. This assignment was supported by 2D NMR nOe experiments.

Photophysical Measurements. The absorption spectra were recorded in EtOH/MeOH (4:1 by volume) or CH_2Cl_2/MeOH 1:1 by volume (**8** as the PF_6 salt), using a Varian Cary 5E UV/vis/near-IR spectrophotometer. For the temperature-dependent emission properties, the samples were placed in quartz ampules (diameter 5 mm) which were purged with N_2 and sealed. The solvent vitrifies to a glass in the 130−110 K region. The ampules were placed in a liquid-nitrogen-cooled Oxford Instruments ND 1704 cryostat with a temperature control unit.

Emission spectra and quantum yields were determined using a SPEX Fluorolog 2 spectrofluorimeter using an excitation wavelength of 452 nm and right-angle detection. Correction factors for the wavelength-dependent sensitivity of the detection system were obtained using a lamp (General Electric DXW, 1000 W) calibrated by the Swedish National Testing and Research Institute.[34]

For each complex, the temperature dependence of the quantum yield was determined in one series of measurements on the same sample, without changing the sample position. The values thus obtained were calibrated at 100 K against [Ru(bpy)$_3$]$^{2+}$, using samples with an absorbance of 0.100 at 452 nm (determined at 298 K) in a 1 cm rectangular cuvette. The cuvette could be accurately repositioned after removal from the cryostat, ensuring correct calibration. A value[1a] of Φ_{em} = 0.38 at 77 K was used for [Ru(bpy)$_3$]$^{2+}$. It was assumed that the differences in optical density and index of refraction for temperatures above the glass transition cancelled within experimental error.[29a] It was also assumed that the solvent contracted to 80% of its volume upon vitrification, resulting in an increased concentration, and the apparent values of Φ_{em} were corrected accordingly. It must be emphasized that the uncertainties of absolute quantum yields are generally assumed to be at least 20%.[35] Also, relative quantum yields should be considered with caution when changes in the solvent state occur, such as in the present case.

Emission lifetimes were determined using an N_2 laser (LSI Laser Science, Inc., Model VSL 337ND, λ = 337 nm, pulse width $\approx$ 10 ns) or an excimer laser (Lambda Physics EMG 100, with XeCl, λ = 308 nm, pulse width $\approx$ 15 ns). A Tektronix 7912 AD digitizer was used in the detector system.

No sign of decomposition of the complexes was seen during the photophysical measurements.

(34) Norden, B.; Seth, S. *Appl. Spectrosc.* **1985**, *39*, 647.
(35) Demas, J. N.; Crosby, G. A. *J. Phys. Chem.* **1971**, *75*, 991.

Table 5. Crystallographic Data for **5**

formula (X-ray study)	$RuC_{22}H_{14}N_4O_4 \cdot C_2H_5OH$
fw	545.55
unit cell dimens	$a = 11.088(3)$ Å
	$b = 11.226(3)$ Å
	$c = 35.283(9)$ Å
	$\alpha = \gamma = 90°$, $\beta = 91.41(2)°$
unit cell vol, V	4390(2) Å^3
formula units/unit cell, Z	8
space group	$P2_1/n$ (No. 14)
temp, T	293 K
wavelength, λ(Cu Kα)	1.54184 Å
calcd density, D_x	1.65 g·cm^{-3}
linear abs coeff	62 cm^{-1}
$R(F)^a$ for obsd reflns	0.057
$R_w(F)^b$ for obsd reflns	0.068

^{a} $R(F) = \sum(F_o| - |F_c|)/\sum|F_o|$. ^{b} $R_w(F) = [\sum w(|F_o| - |F_c|)^2/\sum w|F_o|^2]^{1/2}$ where $w = 1/\sigma^2(|F_o| + 0.0008F_o^2)$.

Electrochemical Measurements. Reduction potentials were determined using cyclic voltammetry in acetonitrile (anhydrous, <0.005% water, in Aldrich Sure/Seal bottles) with 0.1 M Bu_4NBF_4. The acetonitrile was syringe-transferred to a nitrogen-flushed cell containing the electrolyte salt and the complex. A three-electrode system with glassy-carbon (working), platinum-wire (counter), and calomel (SCE, reference) electrodes was used. The porous glass plug of the SCE was rinsed with water between each experiment to avoid precipitation of salt due to acetonitrile entering the plug. It is important to note that a significant junction potential exists between acetonitrile and water in the SCE. As a consequence, the reduction potentials reported for $[Ru(bpy)_3]^{2+}$ vs SCE in acetonitrile[21] and vs NHE in water[36] are very similar. The junction potential could be kept constant, which was carefully checked, and allowed meaningful comparison between different complexes. Our values for the peak potentials of $[Ru(bpy)_3]^{2+}$ were in excellent agreement with previous reports.[21]

Single-Crystal X-ray Diffraction. The structure of **5** was determined by single-crystal X-ray diffraction using Cu Kα, $\lambda = 1.541\,84$ Å, radiation at 293 K. The compound crystallizes in the monoclinic space group $P2_1/n$ with $Z = 8$. The unit cell dimensions are $a = 11.088(3)$ Å, $b = 11.226(3)$ Å, $c = 35.283(9)$ Å, $\beta = 91.41(2)°$, and $V = 4390(2)$ Å^3. The structure was refined to $R_w = 0.068$ for 2635 observed reflections with $I > 3\sigma_I$. Two disordered ethanol molecules were present in the structure.

A suitable, dark red crystal of **5** was mounted on a STOE four-circle single-crystal diffractometer using graphite-monochromatized Cu Kα radiation. Accurate unit cell parameters were obtained by a least-squares refinement, using the observed θ angles of 18 well-centered reflections selected in the range $20.3° < 2\theta < 34.9°$. Intensity data collection was performed at 293 K for 7011 reflections. The collected data were corrected for background, Lorentz−polarization, and absorption effects. The systematic absences in the collected data agree with the space group symmetry $P2_1/n$. The initial position of the Ru atom was derived by the interpretation of a Patterson map. The positions of the non-hydrogen atoms were located by subsequent difference electron density ($\Delta\rho$) maps and refined by full-matrix least-squares techniques. The hydrogen atoms were initially located at idealized positions, which were then refined by assigning the hydrogens the same thermal parameters as those of their parent carbon atoms. The distance to the parent carbon was set to 1.08 Å. The non-hydrogen atom positions of two slightly disordered ethanol molecules per asymmetric unit, found from $\Delta\rho$ maps, were refined with the thermal parameter fixed to 0.2. The positions of the ethanolic oxygen atoms and carbon atoms were refined under the constraints that carbon atoms and oxygen atoms had common fixed thermal parameters and common oxygen−carbon and carbon−carbon bond lengths. No hydrogen atoms for these ethanol molecules were located. The refined oxygen−carbon and carbon−carbon bond lengths became about 1.5 Å. In the final refinement cycles, the positions of the O and C atoms in the ethanol molecules were kept fixed to improve the overall convergence. With anisotropic thermal parameters for the ruthenium, oxygen (except for the two ethanol oxygen atoms), and nitrogen atoms, the R value for 2635 observed reflection became 0.057 ($R_w = 0.068$). (See Table 5.)

Selected bond lengths and bond angles for the coordination polyhedron around ruthenium are given in Table 4. A table of calculated least-square planes is given in SI Table S1. The crystallographic calculations were performed using the SHELX-76 computer program package.[37] Geometrical calculations and ORTEP plotting were performed using PLATON.[38] The computer programs for correction of absorption effects and for molecular superposition by least-squares techniques were written by R.N.[39] Atomic scattering factors with anomalous dispersion corrections were taken from ref 40.[40]

Acknowledgment. This is Publication No. 9 from the Consortium for Studies of Artificial Photosynthesis, supported financially by the Knut and Alice Wallenberg Foundation. This work was also supported by the NFR (Swedish Natural Science Research Council) and NUTEK (Swedish National Board for Industrial and Technical Development). T.N. acknowledges a personal grant from Vattenfall AB, Sweden.

Supporting Information Available: ESI-MS spectra (experimental and simulated) of compounds **5**, **6**, **7**, **9**, and **11**, and a unit cell packing diagram and a table of calculated least-square planes for **5** (7 pages). One crystallographic file, in CIF format, is available for compound **5** on the Internet only. Ordering and access information is given on any current masthead page.

IC9705812

(36) Lytle, F. E.; Hercules, D. M. *Photochem. Photobiol.* **1971**, *13*, 123.

(37) Sheldrick, G. M. SHELX76, Program for Crystal Structure Determination. University of Cambridge, 1976.

(38) Spek, A. L. PLATON-96. Utrecht University, 3584 CH Utrecht, The Netherlands, 1996.

(39) (a) Norrestam, R. STOEABS, Program for analytical absorption corrections. Personal communication. (b) Norrestam, R. ROTPLOT, Program for molecular superposition by least squares techniques. Personal communication.

(40) *International Tables for X-ray Crystallography*; Kynoch: Birmingham, U.K., 1974; Vol. 4.